

## 3D PRINTED LATTICES WITH SPATIALLY VARIANT SELF-COLLIMATION

Raymond C. Rumpf<sup>1, \*</sup>, Javier Pazos<sup>1</sup>, Cesar R. Garcia<sup>1</sup>, Luis Ochoa<sup>2</sup>, and Ryan Wicker<sup>2</sup>

<sup>1</sup>EM Lab, W. M. Keck Center for 3D Innovation, University of Texas at El Paso, El Paso, Texas 79968, USA

<sup>2</sup>W. M. Keck Center for 3D Innovation, University of Texas at El Paso, El Paso, Texas 79968, USA

**Abstract**—In this work, results are given for controlling waves arbitrarily inside a lattice with spatially variant self-collimation. To demonstrate the concept, an unguided beam was made to flow around a 90° bend without scattering due to the bend or the spatial variance. Control of the field was achieved by spatially varying the orientation of the unit cells throughout a self-collimating photonic crystal, but in a manner that almost completely eliminated deformations to the size and shape of the unit cells. The device was all-dielectric, monolithic, and made from an ordinary dielectric with low relative permittivity ( $\epsilon_r = 2.45$ ). It was manufactured by fused deposition modeling, a form of 3D printing, and its performance confirmed experimentally at around 15 GHz.

### 1. INTRODUCTION

Metamaterials and photonic crystals are engineered composites that exhibit superior properties not found in nature and that are not observed in the constituent materials [1]. They are composed of a periodic lattice of physical features that interact with an applied wave to produce new and useful phenomena including negative refractive index [2–4], dispersive properties [5–11], electromagnetic band gaps [12–15], anisotropy [16–27], and more. All of these phenomena depend strongly on the direction of an applied wave and/or the polarization of the field. In addition, electromagnetic waves cannot be controlled using homogeneous materials. Functional

---

*Received 5 March 2013, Accepted 28 March 2013, Scheduled 17 April 2013*

\* Corresponding author: Raymond C. Rumpf (rcrumpf@utep.edu).

devices must contain inhomogeneous features like material interfaces, curved surfaces, or gradients. It is therefore necessary to spatially vary the geometric attributes of a lattice in order to: (1) exploit directional phenomena, and/or (2) make the lattices macroscopically inhomogeneous. Spatial variance, however, must be incorporated in a manner that does not degrade performance by deforming the geometry of the unit cells. It should also be noted that a major problem in traditional metamaterials is the prohibitively high loss caused by metallic resonators [28–32]. Loss is very often orders of magnitude larger than what can be tolerated by the application. The extensive use of metals in traditional metamaterials also makes them less viable for specialized applications at high power [33–36] or at high temperatures [37] where problems with loss, heat, arcing, and chemical reactivity are more pronounced. All-dielectric metamaterials and photonic crystals hold great promise to solve these problems, but dielectrics exhibit a weaker interaction with the field so design options are more limited. This can be partly overcome through clever engineering of the dispersion and anisotropy of the dielectric structures. This, however, usually leads to devices with highly complex geometries that are not feasible to manufacture by conventional means. In these regards, 3D printing seems ideally suited for producing the next generation of electromagnetic devices that will have complex geometries and will likely make heavier use of sculpted dielectrics.

In the present work, we demonstrate a spatially variant all-dielectric photonic crystal as a new method for spatial control of electromagnetic waves in 3D systems. The final device, shown in Figure 1, exploits the directional properties of self-collimation to perform the simple task of flowing an unguided beam around a  $90^\circ$

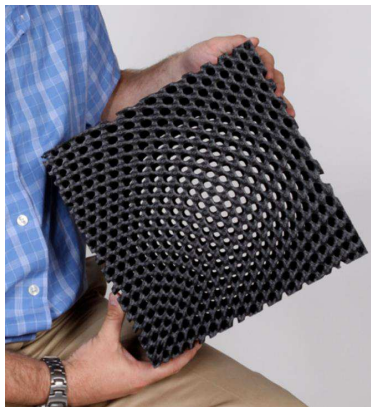


**Figure 1.** Photograph of the spatially variant self-collimating lattice.

bend without diffracting or scattering. Self-collimation [38–44] is a phenomenon where a beam propagates without diffraction and is forced to flow in a specific direction relative to the principal axes of the unit cells. Using this effect, a beam can be made to flow along an arbitrarily curved path by spatially varying the orientation of the unit cells. Devices based on self-collimation can be monolithic, all-dielectric, and composed of just ordinary isotropic materials. Our experience has shown that such devices are also highly tolerant to dielectric loss and to surface roughness. Excellent performance can even be obtained using materials with low dielectric constant (i.e.,  $\varepsilon_r < 3.0$ ) that are usually less expensive and more commonly available than more exotic dielectrics with higher permittivity. Alternative techniques for spatial control of waves within a lattice include structures produced by transformation optics [45], waveguides [46, 47], graded-index devices [48–50], introduction of defects [43], and graded photonic crystals [51–55]. Spatially-variant self-collimation is unique because it spatially varies the orientation of the unit cells within an otherwise monolithic and uniform lattice. Devices can often be designed with fewer lattice periods and with lower dielectric contrast than with the alternative approaches. No extreme or anisotropic constitutive parameters are needed. Other degrees of freedom like fill fraction and lattice spacing can be spatially varied at the same time for optimizing a design or building in additional functionality. The device presented in this paper is not a waveguide and it cannot be designed using transformation optics because the unit cells are isotropic and their fill fraction is kept uniform throughout the lattice.

## 2. DEVICE DESIGN

We began our design with a unit cell described by the superposition of just three planar gratings. This description was chosen to speed the procedure of spatially varying the lattice [56]. The grating vectors describing the three planar gratings were chosen to produce a lattice with simple cubic symmetry as follows:  $\mathbf{K}_1 = \mathbf{a}_x 2\pi/\Lambda$ ,  $\mathbf{K}_2 = \mathbf{a}_y 2\pi/\Lambda$ , and  $\mathbf{K}_3 = \mathbf{a}_z 2\pi/\Lambda$ . Given these, the unit cell as a function of position  $\mathbf{r}$  was constructed according to Eq. (1) by adding the three gratings and then applying a threshold to define regions as either just air or dielectric. To generate a unit cell with 30% fill fraction of dielectric, the threshold parameter was set to  $\gamma = 0.6165$ .

$$\varepsilon_r(\mathbf{r}) = \begin{cases} 1.0 & \varepsilon'_r(\mathbf{r}) \leq \gamma \\ \varepsilon_{uc} & \varepsilon'_r(\mathbf{r}) > \gamma \end{cases} \quad (1)$$

$$\varepsilon'_r(\mathbf{r}) = \cos(\mathbf{K}_1 \cdot \mathbf{r}) + \cos(\mathbf{K}_2 \cdot \mathbf{r}) + \cos(\mathbf{K}_3 \cdot \mathbf{r})$$

The device was manufactured using a polycarbonate-ABS blend (310-20500 filament from Stratasys) which was measured to have a dielectric constant of  $\epsilon_{uc} = 2.45$  at 15 GHz. The loss tangent of the material was ignored in the design, but it was measured to be  $\tan \delta = 0.04$  at this same frequency. The lattice spacing was chosen to be  $\Lambda = 1.59$  cm to place the center frequency of self-collimation at around 15 GHz. The resulting unit cell is shown in Figure 2.

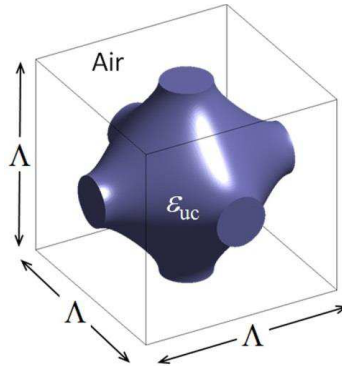


**Figure 2.** Three-dimensional simple cubic unit cell with 30% fill fraction.

The unit cell was analyzed for self-collimation using the concept of isofrequency contours (IFCs) [39, 41]. These were calculated using the reduced Bloch mode expansion technique [57] based on the plane wave expansion method [58, 59]. IFCs are dispersion surfaces in  $k$ -space that characterize the magnitude of the wave vector as a function of the direction of a Bloch wave propagating through a uniform infinite lattice. Given a point on an IFC, phase propagates according to the wave vector that extends from the origin to that point. In contrast, energy propagates according to the Poynting vector that is in a direction normal to the surface of the IFC at that point. In ordinary isotropic materials, the IFCs are spherical and phase and energy propagate in the same direction. In photonic crystals the IFCs can be engineered to take on other shapes, usually resembling the shape of the Brillouin zone. In these cases, the energy and phase of a wave can propagate in different directions. Self-collimation occurs when a portion of the IFC is flat and energy is forced to flow in a common direction over an entire span of wave vectors. Only small portions of the IFC are truly flat, however, and Fourier components of a beam that lie outside the flat regions will diverge, but much more slowly than they would outside of the lattice. The severity of the divergence

depends on the slope of the IFC. In addition, when the beam exits the lattice it is no longer self-collimated and will diverge or diffract according to whatever amplitude and phase distribution is imparted on the beam.

We define the “region of self-collimation” as the span of angles and frequencies in  $k$ -space over which the Poynting vectors are parallel to within some threshold angle  $\theta$ . We estimated this threshold by requiring that no energy in the beam be offset laterally by more than half of the beam width  $w$  after propagating through the entire lattice. If the beam must travel a total distance of  $L$ , the angle tolerance should be set to  $\tan \theta = w/(2L)$ . In the present device, the beam travels a total distance of 19.7 unit cells and through simulation we assessed the beam width to be around 6 unit cells inside the lattice. Based on these quantities, our angle tolerance was calculated to be  $\theta = 8.7^\circ$ . From this, we define the field-of-view (FOV) of the self-collimation effect to be the solid angle that bounds the region of self-collimation. We further define the bandwidth of the self-collimation effect to be the range of frequencies over which the IFCs remain flat to within this same tolerance. Figure 3 shows the 3D IFC calculated at 15.2 GHz as well as a cross section of all the IFCs throughout the entire Brillouin zone. The 3D IFC at the center of this figure is shaped like a cube with rounded corners and a large portion of each face is flat to within our threshold. The FOV enclosing the flat region on the IFC is shown as a rounded square cone emanating from the origin. From this data, the FOV was predicted to be  $52.5^\circ$ , and it was maintained over a fractional bandwidth of 6.1% (915 MHz). The FOV can be considerably larger over narrower bandwidths. A consequence of the IFC resembling a

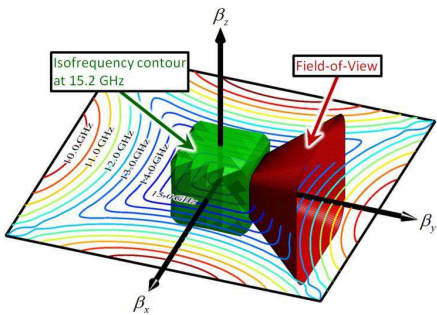


**Figure 3.** Isofrequency contours superimposed with field-of-view.

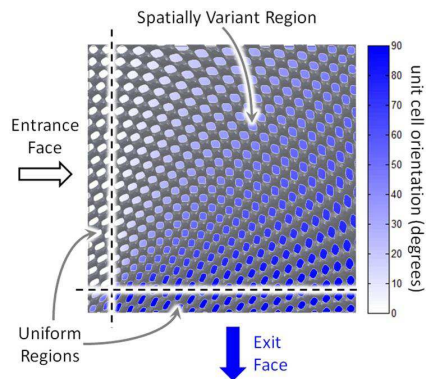


**Figure 4.** Final lattice superimposed on top of the orientation function.

cube is that the lattice has the ability to self-collimate along three different axes. If defects are introduced into the lattice, power can be scattered into these other directions. The scattering can be suppressed somewhat by tailoring the symmetry of the unit cells, but this was not done here because no defects were introduced and the spatial variance was kept sufficiently smooth.

Given this unit cell design, we generated the geometry of the spatially variant lattice to flow a beam around a  $90^\circ$  bend. To do this, we used a novel algorithm capable of spatially varying all of the attributes of a lattice independently and simultaneously while still rendering the overall lattice smooth and continuous [56]. Attributes include unit cell orientation, lattice spacing, fill fraction, geometry, material composition, and more. The present design called only for the orientation of the unit cells to be gradually rotated by  $90^\circ$  in an azimuthal pattern, as illustrated in Figure 4. The arrows outside the lattice identify the entrance and exit faces. As indicated in the figure, the orientation of the unit cells was made constant for two unit cells at the entrance and exit faces to help a beam transition into and out of the bend. The pattern of the orientation function at the extreme inside of the bend was constructed to make the function as smooth and continuous as possible. The synthesis algorithm kept the lattice spacing amazingly uniform despite the orientation of the unit cells being spatially varied and the radius of the curve varying by more than  $20\times$  across the device. This property is very important because fluctuations in the shape and size of the unit cell detune the self-collimation effect.

A basic assumption in the design approach described above is that the lattice is uniform and infinitely periodic. This assumption is no longer true when the lattice is spatially varied. As long as adjacent unit cells are sufficiently similar, however, the resonance and dispersion effects of the lattice can still be maintained to some degree. In the context of IFCs, spatially varying the orientation of the unit cells rotates the IFCs along with the unit cells. In this manner, the directionality of the self-collimation effect is spatially varied so as to flow a beam along a desired path. To assess how abruptly a lattice can be spatially varied while still maintaining self-collimation, a series of simulations was performed for differently sized lattices using the finite-difference frequency-domain method [60]. The confinement of the beam around the bends was evaluated visually. Results from this study are shown in Figure 5. While lattices as small as  $12 \times 12$  unit cells performed reasonably well, it was decided to manufacture the final lattice with  $22 \times 22 \times 11$  unit cells as a safety margin. The 3D geometry was exported from the synthesis tool as an industry standard STL file.

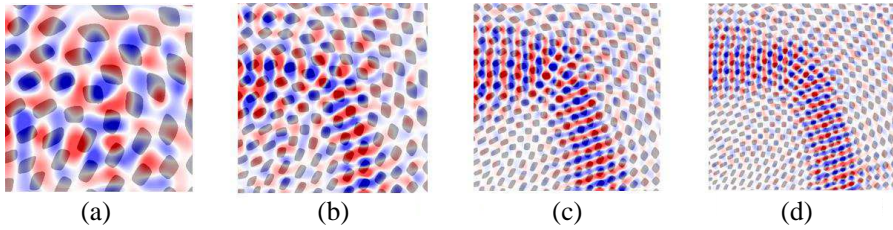


**Figure 5.** Simulations of lattices with different sizes to determine the minimum bend radius. (a)  $7 \times 7$  unit cells. (b)  $12 \times 12$  unit cells. (c)  $17 \times 17$  unit cells. (d)  $22 \times 22$  unit cells.

### 3. EXPERIMENTAL RESULTS

3D printing is ideally suited for manufacturing devices with complex geometries. It provides the ability to arbitrarily place different materials in three dimensions with high precision [61, 62]. 3D printing is already well established for producing rapid prototypes, but recent advances in equipment and materials have made it viable for producing functional devices and even final products [63–69]. The device presented here was printed from the STL file using fused deposition modeling (FDM) in a Stratasys FDM 400 mc. FDM was inspired by the hot glue gun and feeds an inexpensive thermoplastic filament through a print head where it is melted and deposited onto the surface of a platform. The print head is translated within the horizontal plane to deposit a layer of the material in the desired pattern. When a layer is finished, the platform is lowered by a few thousandths of an inch and the next layer is written on top of the previous. This process is repeated layer-by-layer to produce a fully three-dimensional structure. Printed parts are typically built with temporary support material to prevent sagging of the hot plastic. It was determined that our device could be printed without using support material, which would have been difficult to remove from the internal features of the device. Building without support cannot always be achieved, but in this case the lattice features were self-supporting when the fill fraction was set to 30%. The final device, shown in Figure 1, took approximately two weeks to build.

To measure the device's performance in the laboratory and confirm its operation, the lattice was placed onto a Styrofoam platform and illuminated at the entrance face by a standard gain horn antenna operating within the Ku-band (12 GHz to 18 GHz). A field probe was constructed from a small monopole antenna and scanned around the perimeter of the device to profile the field. 44 samples were taken along each of the three sides for a total of 132 points. The data was captured

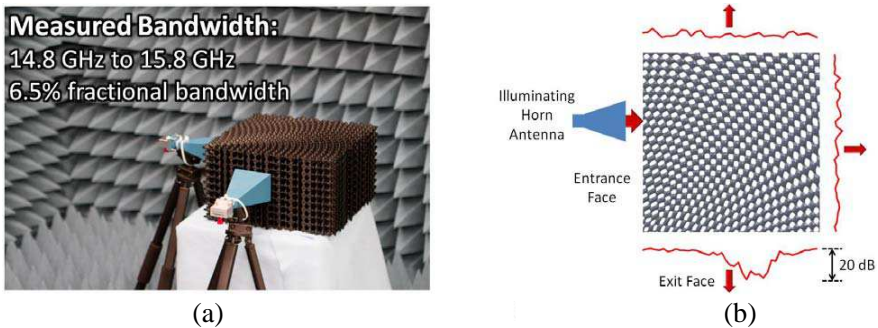


**Figure 6.** Experimental results for the spatially variant self-collimating lattice. (a) Spatially variant lattice in test setup. (b) Measured field profile around perimeter of device.

using an Agilent N5245 PNA-X vector network analyzer. Figure 6(a) shows a photograph of the device in its test configuration. Figure 6(b) shows the field amplitude data measured at 15.2 GHz plotted around the perimeter of the device where it was measured.

It was observed experimentally that the device self-collimated from 14.8 GHz up to 15.8 GHz, exhibiting a 6.5% fractional bandwidth. We measured approximately a 20 dB (99%) fluctuation in the field amplitude in the location of the exiting beam. The mismatch between air and the lattice produced some scattering from the edges of the device. Techniques have been developed to overcome this [70, 71], but they were not implemented here. Waves scattered by the entrance face did not affect the measurements. The noise in our measured results was caused by the waves scattered from the exit face. These waves were reflected backwards into the device in multiple directions and eventually exited all of the faces. This scattering was observed in the simulations as well. Despite this, the exiting beam is obvious and the data confirms the device's operation.

#### 4. CONCLUSION

This paper presented experimental results of an all-dielectric spatially variant photonic crystal that flowed an unguided beam around a  $90^\circ$  bend without diffracting or scattering. It is the first known effort to exploit the directional dependence of self-collimation by spatially varying the orientation of the unit cells throughout a lattice. The all-dielectric design eliminated the loss problems associated with traditional metallic metamaterials. This makes the technology

attractive for integrated optics such as silicon photonics, as well as specialized applications at high power and at ultra-high temperatures where metals can be problematic. Excellent performance was achieved because the final lattice was defect-free, lattice spacing was kept strikingly uniform, and it was manufactured very well by 3D printing. The concepts demonstrated by this device, and their many variations, provide new mechanisms for controlling electromagnetic waves. Due to the size scale, most applications of self-collimation will be in the millimeter wave to optical frequencies and may include switching, fan out devices, coupling circuits, spectroscopy, creating quiet zones for antennas or sensors, modifying the radiation patterns of antennas, shaping beams, manipulating images, energy collection, and more. Future work will entail more complex spatial variance, incorporating structures to prevent scattering at the edges of the device, and spatially varying other phenomena.

## ACKNOWLEDGMENT

This work was supported, in part, by DARPA through a 2011 Young Faculty Award.

## REFERENCES

1. Capolino, F., *Theory and Phenomena of Metamaterials*, 1st Edition, CRC Press, 2009.
2. Shelby, R., D. Smith, and S. Schultz, "Experimental verification of a negative index of refraction," *Science*, Vol. 292, 77–79, 2001.
3. Smith, D. R., J. B. Pendry, and M. C. K. Wiltshire, "Metamaterials and negative refractive index," *Science*, Vol. 305, 788–792, 2004.
4. Smith, D. R. and N. Kroll, "Negative refractive index in left-handed materials," *Physical Review Letters*, Vol. 85, 2933–2936, 2000.
5. Gralak, B., S. Enoch, and G. Tayeb, "Anomalous refractive properties of photonic crystals," *JOSA A*, Vol. 17, 1012–1020, 2000.
6. Wu, L., M. Mazilu, and T. F. Krauss, "Beam steering in planar-photonic crystals: From superprism to supercollimator," *Journal of Lightwave Technology*, Vol. 21, 561, 2003.
7. Notomi, M., "Negative refraction in photonic crystals," *Optical and Quantum Electronics*, Vol. 34, 133–143, 2002.

8. Baba, T. and M. Nakamura, "Photonic crystal light deflection devices using the superprism effect," *IEEE Journal of Quantum Electronics*, Vol. 38, 909–914, 2002.
9. Enoch, S., G. Tayeb, and B. Gralak, "The richness of the dispersion relation of electromagnetic bandgap materials," *IEEE Transactions on Antennas and Propagation*, Vol. 51, 2659–2666, 2003.
10. Baba, T., "Slow light in photonic crystals," *Nature Photonics*, Vol. 2, 465–473, 2008.
11. Kosaka, H., T. Kawashima, A. Tomita, M. Notomi, T. Tamamura, T. Sato, and S. Kawakami, "Superprism phenomena in photonic crystals: Toward microscale lightwave circuits," *Journal of Lightwave Technology*, Vol. 17, 2032, 1999.
12. Yablonovitch, E., "Inhibited spontaneous emission in solid-state physics and electronics," *Physical Review Letters*, Vol. 58, 2059–2062, 1987.
13. Yablonovitch, E., "Photonic crystals," *Journal of Modern Optics*, Vol. 41, 173–194, 1994.
14. John, S., "Strong localization of photons in certain disordered dielectric superlattices," *Physical Review Letters*, Vol. 58, 2486–2489, 1987.
15. Noda, S., A. Chutinan, and M. Imada, "Trapping and emission of photons by a single defect in a photonic bandgap structure," *Nature*, Vol. 407, 608–610, 2000.
16. Grann, E. B., M. Moharam, and D. A. Pommet, "Artificial uniaxial and biaxial dielectrics with use of two-dimensional subwavelength binary gratings," *JOSA A*, Vol. 11, 2695–2703, 1994.
17. Lindell, I., S. Tretyakov, K. Nikoskinen, and S. Ilvonen, "BW media — Media with negative parameters, capable of supporting backward waves," *Microwave and Optical Technology Letters*, Vol. 31, 129–133, 2001.
18. Smith, D. and D. Schurig, "Electromagnetic wave propagation in media with indefinite permittivity and permeability tensors," *Physical Review Letters*, Vol. 90, 77405, 2003.
19. Smith, D. R., P. Rye, D. C. Vier, A. F. Starr, J. J. Mock, and T. Perram, "Design and measurement of anisotropic metamaterials that exhibit negative refraction," *IEICE Transactions on Electronics*, Vol. E87-C, 359–370, 2004.
20. Smith, D. R., D. Schurig, J. J. Mock, P. Kolinko, and P. Rye, "Partial focusing of radiation by a slab of indefinite media,"

- Applied Physics Letters*, Vol. 84, 2244, 2004.
21. Wood, B., J. Pendry, and D. Tsai, "Directed subwavelength imaging using a layered metal-dielectric system," *Physical Review B*, Vol. 74, 115116, 2006.
  22. Hao, J., Y. Yuan, L. Ran, T. Jiang, J. A. Kong, C. Chan, and L. Zhou, "Manipulating electromagnetic wave polarizations by anisotropic metamaterials," *Physical Review Letters*, Vol. 99, 63908, 2007.
  23. Hoffman, A. J., L. Alekseyev, S. S. Howard, K. J. Franz, D. Wasserman, V. A. Podolskiy, E. E. Narimanov, D. L. Sivco, and C. Gmachl, "Negative refraction in semiconductor metamaterials," *Nature Materials*, Vol. 6, 946–950, 2007.
  24. Elser, J. and V. A. Podolskiy, "Scattering-free plasmonic optics with anisotropic metamaterials," *Physical Review Letters*, Vol. 100, 66402, 2008.
  25. Yao, J., Z. Liu, Y. Liu, Y. Wang, C. Sun, G. Bartal, A. M. Stacy, and X. Zhang, "Optical negative refraction in bulk metamaterials of nanowires," *Science*, Vol. 321, 930–930, 2008.
  26. Fang, A., T. Koschny, and C. M. Soukoulis, "Optical anisotropic metamaterials: Negative refraction and focusing," *Physical Review B*, Vol. 79, 245127, 2009.
  27. Garcia, C. R., J. Correa, D. Espalin, J. H. Barton, R. C. Rumpf, R. Wicker, and V. Gonzalez, "3D printing of anisotropic metamaterials," *Progress In Electromagnetics Research Letters*, Vol. 34, 75–82, 2012.
  28. Ponizovskaya, E., M. Nieto-Vesperinas, and N. Garcia, "Losses for microwave transmission in metamaterials for producing left-handed materials: The strip wires," *Applied Physics Letters*, Vol. 81, 4470–4472, 2002.
  29. Varadan, V. and L. Ji, "Accounting for power 'loss' in metamaterials," *Metamaterials 2008*, Pamplona, Spain, 2008.
  30. Fang, A., T. Koschny, M. Wegener, and C. Soukoulis, "Self-consistent calculation of metamaterials with gain," *Physical Review B*, Vol. 79, 241104, 2009.
  31. Varadan, V. V. and J. Liming, "Does a negative refractive index always result in negative refraction? — Effect of loss," *IEEE MTT-S International Microwave Symposium Digest, MTT' 09*, 61–64, 2009.
  32. Khurgin, J. B. and G. Sun, "Scaling of losses with size and wavelength in nanoplasmonics and metamaterials," *Applied Physics Letters*, Vol. 99, 211106, 2011.

33. De Damborenea, J., "Surface modification of metals by high power lasers," *Surface and Coatings Technology*, Vol. 100, 377–382, 1998.
34. Batanov, G., N. Berezhetskaya, I. Kossyi, A. Magunov, and V. Silakov, "Interaction of high-power microwave beams with metal-dielectric media," *The European Physical Journal Applied Physics*, Vol. 26, 11–16, 2004.
35. Petelin, M. and A. Fix, "Comparison of metals in their steadiness to pulse-periodic microwave heating fatigue," *IEEE International Vacuum Electronics Conference*, 163–164, 2009.
36. Bilik, V. and J. Bezek, "High power limits of waveguide stub tuners," *J. Microw. Power*, Vol. 44, 178–186, 2010.
37. Anžel, I., "High temperature oxidation of metals and alloys," 325–336, Association of Metallurgical Engineers of Serbia, 2007.
38. Kosaka, H., T. Kawashima, A. Tomita, M. Notomi, T. Tamamura, T. Sato, and S. Kawakami, "Self-collimating phenomena in photonic crystals," *Applied Physics Letters*, Vol. 74, 1212, 1999.
39. Witzens, J., M. Loncar, and A. Scherer, "Self-collimation in planar photonic crystals," *IEEE Journal of Selected Topics in Quantum Electronics*, Vol. 8, 1246–1257, 2002.
40. Iliw, R., C. Etrich, U. Peschel, F. Lederer, M. Augustin, H. J. Fuchs, D. Schelle, E. B. Kley, S. Nolte, and A. Tunnermann, "Diffractionless propagation of light in a low-index photonic-crystal film," *Applied Physics Letters*, Vol. 85, 5854–5856, 2004.
41. Feng, S., Z.-Y. Li, Z.-F. Feng, K. Ren, B.-Y. Cheng, and D.-Z. Zhang, "Focusing properties of a rectangular-rod photonic-crystal slab," *Journal of Applied Physics*, Vol. 98, 063102, 2005.
42. Iliw, R., C. Etrich, and F. Lederer, "Self-collimation of light in three-dimensional photonic crystals," *Optics Express*, Vol. 13, 7076–7085, 2005.
43. Shin, J. and S. Fan, "Conditions for self-collimation in three-dimensional photonic crystals," *Optics Letters*, Vol. 30, 2397–2399, 2005.
44. Lu, Z., S. Shi, J. A. Murakowski, G. J. Schneider, C. A. Schuetz, and D. W. Prather, "Experimental demonstration of self-collimation inside a three-dimensional photonic crystal," *Physical Review Letters*, Vol. 96, 173902, 2006.
45. Kwon, D. H. and D. H. Werner, "Transformation optical designs for wave collimators, flat lenses and right-angle bends," *New Journal of Physics*, Vol. 10, 115023, 2008.
46. Mekis, A., J. Chen, I. Kurland, S. Fan, P. R. Villeneuve, and J. Joannopoulos, "High transmission through sharp bends in

- photonic crystal waveguides,” *Physical Review Letters*, Vol. 77, 3787–3790, 1996.
47. Roberts, D., M. Rahm, J. Pendry, and D. Smith, “Transformation-optical design of sharp waveguide bends and corners,” *Applied Physics Letters*, Vol. 93, 251111, 2008.
  48. Gabrielli, L. H. and M. Lipson, “Integrated Luneburg lens via ultra-strong index gradient on silicon,” *Optics Express*, Vol. 19, 20122–20127, 2011.
  49. Spadoti, D. H., L. H. Gabrielli, C. B. Poitras, and M. Lipson, “Focusing light in a curved-space,” *Optics Express*, Vol. 18, 3181–3186, 2010.
  50. Vasic, B., G. Isic, R. Gajic, and K. Hingerl, “Controlling electromagnetic fields with graded photonic crystals in metamaterial regime,” *Optics Express*, Vol. 18, 20321–20333, 2010.
  51. Akmansoy, E., E. Centeno, K. Vynck, D. Cassagne, and J. M. Lourtioz, “Graded photonic crystals curve the flow of light: An experimental demonstration by the mirage effect,” *Applied Physics Letters*, Vol. 92, 133501, 2008.
  52. Cassan, E., K. V. Do, C. Caer, D. Marris-Morini, and L. Vivien, “Short-wavelength light propagation in graded photonic crystals,” *Journal of Lightwave Technology*, Vol. 29, 1937–1943, 2011.
  53. Centeno, E. and D. Cassagne, “Graded photonic crystals,” *Optics Letters*, Vol. 30, 2278–2280, 2005.
  54. Do, K. V., X. Le Roux, D. Marris-Morini, L. Vivien, and E. Cassan, “Experimental demonstration of light bending at optical frequencies using a non-homogenizable graded photonic crystal,” *Optics Express*, Vol. 20, 4776–4783, 2012.
  55. Li, Y. Y., M. Y. Li, P. F. Gu, Z. R. Zheng, and X. Liu, “Graded wavelike two-dimensional photonic crystal made of thin films,” *Applied Optics*, Vol. 47, C70–C74, 2008.
  56. Rumpf, R. C. and J. Pazos, “Synthesis of spatially variant lattices,” *Optics Express*, Vol. 20, 15263–15274, 2012.
  57. Hussein, M. I., “Reduced Bloch mode expansion for periodic media band structure calculations,” *Proceedings of the Royal Society A: Mathematical, Physical and Engineering Science*, Vol. 465, 2825–2848, 2009.
  58. Johnson, S. G. and J. D. Joannopoulos, “Block-iterative frequency-domain methods for Maxwell’s equations in a planewave basis,” *Optics Express*, Vol. 8, 173–190, 2001.
  59. Guo, S. and S. Albin, “Simple plane wave implementation for photonic crystal calculations,” *Optics Express*, Vol. 11, 167–175,

- 2003.
60. Rumpf, R. C., "Simple implementation of arbitrarily shaped total-field/scattered-field regions in finite-difference frequency-domain," *Progress In Electromagnetics Research*, Vol. 36, 221–248, 2012.
  61. Gibson, I., D. W. Rosen, and B. Stucker, *Additive Manufacturing Technologies: Rapid Prototyping to Direct Digital Manufacturing*, 459, Springer, London, New York, 2010.
  62. Wohlers, T., "Wohlers report 2012: Additive manufacturing and 3D printing state of the industry," Annual Worldwide Progress Report, Wohlers Associates, Fort Collins, 2012.
  63. Palmer, J., B. Jokiel, C. Nordquist, B. Kast, C. Atwood, E. Grant, F. Livingston, F. Medina, and R. Wicker, "Miniature RF components enabled by mesoscale rapid manufacturing," 2005.
  64. Palmer, J., B. Jokiel, C. Nordquist, B. Kast, C. Atwood, E. Grant, F. Livingston, F. Medina, and R. Wicker, "Mesoscale RF relay enabled by integrated rapid manufacturing," *Rapid Prototyping Journal*, Vol. 12, 148–155, 2006.
  65. Choi, J. W., E. MacDonald, and R. Wicker, "Multi-material microstereolithography," *The International Journal of Advanced Manufacturing Technology*, Vol. 49, 543–551, 2010.
  66. Choi, J. W., H. C. Kim, and R. Wicker, "Multi-material stereolithography," *Journal of Materials Processing Technology*, Vol. 211, 318–328, 2011.
  67. Choi, J. W., F. Medina, C. Kim, D. Espalin, D. Rodriguez, B. Stucker, and R. Wicker, "Development of a mobile fused deposition modeling system with enhanced manufacturing flexibility," *Journal of Materials Processing Technology*, Vol. 211, 424–432, 2011.
  68. Lopes, A. J., E. MacDonald, and R. B. Wicker, "Integrating stereolithography and direct print technologies for 3D structural electronics fabrication," *Rapid Prototyping Journal*, Vol. 18, 129–143, 2012.
  69. Wicker, R. B. and E. W. MacDonald, "Multi-material, multi-technology stereolithography," *Virtual and Physical Prototyping*, Vol. 7, 181–194, 2012.
  70. Botten, L., T. White, C. M. de Sterke, and R. McPhedran, "Wide-angle coupling into rod-type photonic crystals with ultralow reflectance," *Physical Review E*, Vol. 74, 026603, 2006.
  71. Śigaj, W. and B. Gralak, "Semianalytical design of antireflection gratings for photonic crystals," *Physical Review B*, Vol. 85, 035114, 2012.